Proc. Natl. Acad. Sci. USA
Vol. 91, pp. 878–882, February 1994
Cell Biology

Calcicludine, a venom peptide of the Kunitz-type protease inhibitor family, is a potent blocker of high-threshold Ca^{2+} channels with a high affinity for L-type channels in cerebellar granule neurons

(toxins/Alzheimer disease/trypsin inhibitor)

HUGUES SCHWEITZ, CATHERINE HEURTEAUX, PATRICK BOIS*, DANIELLE MOINIER, GEORGES ROMEY, AND MICHEL LAZDUNSKI†

Institut de Pharmacologie Moléculaire et Cellulaire, 660 Route des Lucioles, Sophia Antipolis, 06560 Valbonne, France

Communicated by Josef Fried, October 8, 1993

ABSTRACT **Calcicludine (CaC) is a 60-amino acid polypeptide from the venom of *Dendroaspis angusticeps*. It is structurally homologous to the Kunitz-type protease inhibitor, to dendrotoxins, which block K^+ channels, and to the protease inhibitor domain of the amyloid β protein that accumulates in Alzheimer disease. Voltage-clamp experiments on a variety of excitable cells have shown that CaC specifically blocks most of the high-threshold Ca^{2+} channels (L-, N-, or P-type) in the 10–100 nM range. Particularly high densities of specific ^{125}I-labeled CaC binding sites were found in the olfactory bulb, in the molecular layer of the dentate gyrus and the stratum oriens of CA3 field in the hippocampal formation, and in the granular layer of the cerebellum. ^{125}I-labeled CaC binds with a high affinity (K_d = 15 pM) to a single class of noninteracting sites in rat olfactory bulb microsomes. The distribution of CaC binding sites in cerebella of three mutant mice (Weaver, Reeler, and Purkinje cell degeneration) clearly shows that the specific high-affinity labeling is associated with granule cells. Electrophysiological experiments on rat cerebellar granule neurons in primary culture have shown that CaC potently blocks the L-type component of the Ca^{2+} current ($K_{0.5}$ = 0.2 nM). Then CaC, in the nanomolar range, appears to be a highly potent blocker of an L-subtype of neuronal Ca^{2+} channels.**

Most vertebrate nervous cells possess multiple types of voltage-dependent Ca^{2+} channels classified on the basis of their biophysical and pharmacological characteristics, as low-voltage-activated (T-type) and high-voltage-activated (HVA) Ca^{2+} channels (L-, N-, and P-type) (1–4). The cardiac L-type Ca^{2+} channel is the target of numerous organic molecules such as 1,4-dihydropyridines (DHPs) (5–7). The N- and P-type Ca^{2+} channels are essentially present in peripheral and central neurons (8). The N-type Ca^{2+} current is specifically blocked by ω-conotoxin (CgTx), a polypeptide isolated from *Conus geographicus* (9–11). The P-type Ca^{2+} current is insensitive to L- and N-type Ca^{2+} channel blockers and is specifically blocked by a polyamine (funnel-web spider toxin) and a polypeptide (ω-Aga-IVA) both extracted from the funnel-web spider *Agelenopsis aperta* (3, 12).

This paper reports the isolation of a toxin, calcicludine (CaC), from the venom of the green mamba *Dendroaspis angusticeps*. This toxin is a potent blocker of all types of HVA Ca^{2+} channels (L-, N-, and P-type). However, L- type Ca^{2+} channels from cerebellar granule cells appear to be the preferential target of CaC.

MATERIALS AND METHODS

Purification of CaC. The crude venom (500 mg) of *D. angusticeps* (Latoxan, Rosans, France) was dissolved in 1% acetic acid and chromatographed onto a Sephadex G50 column. The peptidic fraction was directly loaded onto a TSK (Toyosoda, Japan) SP 5PW (21.5 × 150 mm) column equilibrated with 1% acetic acid. Peptide fractions were then eluted (Fig. 1 *Top*), with a linear gradient from 1% acetic acid to 1 M ammonium acetate at a flow rate of 8 ml/min. The fractions obtained (horizontal bars) were designated A–R. Fraction Q was lyophilized, redissolved in 1 ml of 0.5% trifluoroacetic acid plus 0.9% triethylamine in water, and loaded on a Lichrosorb RP18 7-μm (250 × 10 mm) column (Merck, Darmstadt, Germany) and eluted (Fig. 1 *Middle*) at a flow rate of 3 ml/min with a linear gradient from 10% to 40% of 0.5% trifluoroacetic acid plus 0.9% triethylamine in acetonitrile. Fraction Q1 is CaC.

The primary structure of CaC (Fig. 1 *Bottom*) was determined by Edman degradation of the complete peptide using an Applied Biosystems model 477A microsequencer. The native peptide had no free SH group (measured by *S*-pyridyl ethylation). It was reduced with 2-mercaptoethanol and pyridylethylated with 4-vinylpyridine (13) before sequencing. A molecular weight of 6978.83 was determined by electrospray ionization mass spectrometry, 1 mass unit apart from the value deduced from the sequence.

Cell Preparations. Primary cultures of rat cardiac cells and of skeletal muscle cells from newborn rats or 19-day-old mouse embryos were prepared as described (14, 15). Chicken dorsal root ganglion (DRG) neurons were dissected from 12- to 15-day-old chicken embryos (16). Rat DRG neurons were dissected from 2- to 5-day postnatal pups. Primary cultures of cerebellar Purkinje and granule cells were prepared as described (17, 18).

Electrophysiology. Ca^{2+} currents were recorded with the whole-cell configuration of the patch-clamp technique (19). The pipette solution contained 140 mM CsCl, 5 mM EGTA, 4 mM $MgCl_2$, 3 mM NaATP buffered at pH 7.3 with 10 mM Hepes·CsOH. External solution with Ca^{2+} contained 140 mM tetraethylammonium (TEA) chloride, 2 mM $CaCl_2$, 1 mM $MgCl_2$, 5 mM glucose buffered at pH 7.4 with 10 mM Hepes·TEA hydroxide. External solutions with Ba^{2+} contained either 5 or 20 mM $BaCl_2$. The mechanical activity of skeletal muscle in primary culture was recorded simultaneously with the electrical activity using a video camera associated with an image analyzer. Contraction measurements on isolated organs were carried out as described (20).

The publication costs of this article were defrayed in part by page charge payment. This article must therefore be hereby marked "*advertisement*" in accordance with 18 U.S.C. §1734 solely to indicate this fact.

Abbreviations: HVA, high-voltage activated; DHP, 1,4-dihydropyridine; CaC, calcicludine; DRG, dorsal root ganglion; PN, PN 200-110; CgTx, ω-conotoxin; APPI, protease inhibitor domain of amyloid β protein.

*Present address: Laboratoire de Physiologie Générale, Centre National de la Recherche Scientifique, Unité Associée 290, 40 Avenue du Recteur Pineau, 86022 Poitiers Cedex, France.
†To whom reprint requests should be addressed.

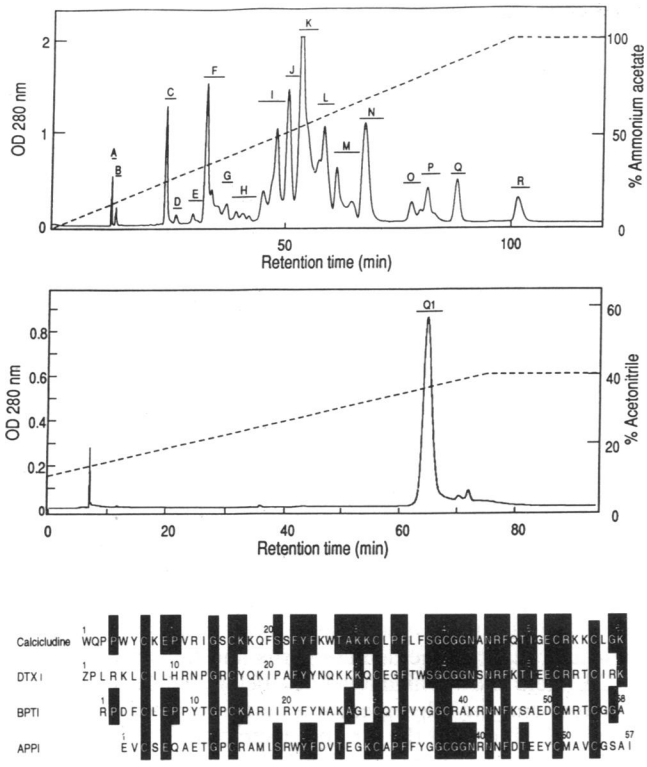

FIG. 1. Purification of CaC (peptide Q) from *D. angusticeps*. (*Top*) HPLC on a TSK SP 5PW column of 200 mg of the peptidic fraction. (*Middle*) Purification by reverse-phase chromatography on a Lichrosorb RP18 column of fraction Q. Peptide Q1 (CaC) is the main peak. (*Bottom*) Sequence homologies between CaC and some protease inhibitors. Homologies are 40% with dendrotoxin I (DTX_I), 29% with the basic pancreatic trypsin inhibitor (BPTI), and 39% with the protease inhibitor domain of the amyloid β protein (APPI).

Iodination of CaC. CaC was iodinated by the Iodo-Gen method (Pierce). Two nanomoles were mixed with 0.5 nmol of $Na^{125}I$ (2000 Ci/mmol; 1 Ci = 37 GBq; NEN) and buffered at pH 7.5 with 100 mM Tris·HCl in an Eppendorf tube coated with 3 nmol of Iodo-Gen (total vol, 40 μl). After a 15-min incubation, free iodine was quenched with 1 ml of bovine serum albumin (BSA) in 20 mM Tris·HCl buffer at pH 8.5 and loaded in a TSK SP 5PW (7.5 × 75 mm) Beckman column. The material was eluted at 1 ml/min with a gradient from 0 to 500 mM NaCl in the same buffer.

Binding to Membranes. Protein concentrations were determined by the Bio-Rad assay with BSA used as a standard. Earle's medium was used for incubations. Incubations were carried out at 25°C for 1 hr, and the samples were diluted with 2 ml of cold washing buffer (wb) (100 mM NaCl/20 mM Tris·HCl, pH 7.4) and filtered on Whatman GF/C filters presoaked with 0.3% polyethylenimine (pH 7.4) and washed with 5 ml of wb before use. The samples were washed twice with 5 ml of wb and the radioactivity retained on the filters was counted.

Autoradiographic Procedures. The homozygous mutant mice used were Weaver (*wv/wv*), Purkinje cell degeneration (*pcd/pcd*), and Reeler (*rl/rl*) mice. Wild-type mice included C57/CBA for Weaver, C57BL/6 for Purkinje cell degeneration, and BALB/c for Reeler. The ages of the mice were 24 days for *wv/wv*, 32 days for *pcd/pcd*, 11 months for *rl/rl*, and similar ages for the corresponding genetic backgrounds. Brain sections were prepared as described (21). Twelve-micrometer-thick frozen brain sections were incubated for 75 min at 20°C in 35 pM ^{125}I-labeled CaC (^{125}I-CaC) dissolved in Earle's medium complemented with BSA (2 mg/ml). Autoradiograms were generated by apposing the labeled tissue to Hyperfilm-^3H (Amersham) for 10 days.

Chemicals. (+)PN 200-110 (PN) was a gift from Sandoz, *d-cis*-diltiazem was from Synthelabo (Bagneux, France), D600 was from Knoll (Liestal, Switzerland), fluspirilene was from Janssen, HOE166 was from Hoechst, and SR 33557 was a gift from Sanofi (Paris); (+)-[*methyl*-^3H]PN 200-110 was purchased from Amersham.

RESULTS

CaC is a 60-amino acid polypeptide with six cysteines forming three disulfide bridges (Fig. 1). Despite its structural homology with dendrotoxins (Fig. 1), which selectively block a class of voltage-dependent K^+ channels (22, 23), CaC, even at high concentration (1 μM), had no effect on dendrotoxin-sensitive K^+ channels in chicken and rat DRG neurons (data not shown). Voltage-dependent Na^+ and K^+ channels of cardiac, skeletal muscle, and neuronal cells were not affected by CaC (1 μM) (data not shown).

CaC depressed cardiac contractibility (Fig. 2*A*) with an EC_{50} value for inhibition of 15 nM (Fig. 2*B*). Cardiac cells express both L- and T-type Ca^{2+} currents (24–26). Since T and L channels activate at very different potentials (−60 and −20 mV, respectively), the effects of CaC on T- and L-type

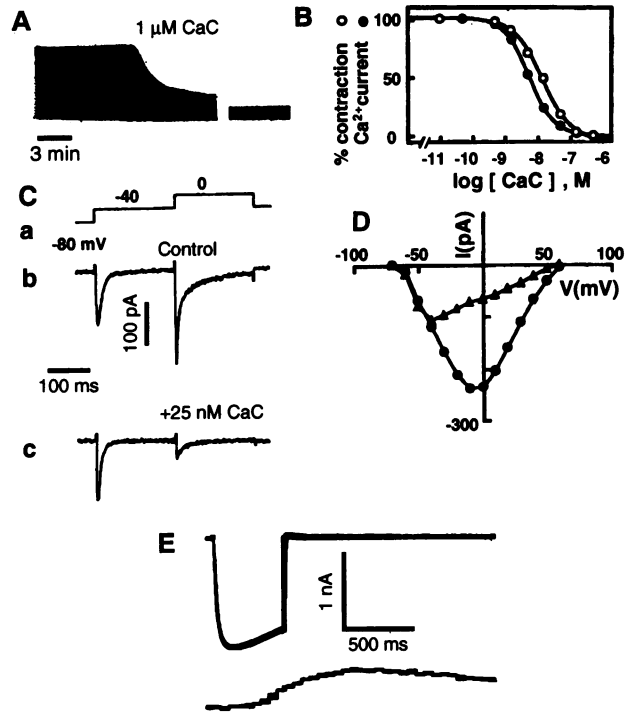

FIG. 2. Effect of CaC on cardiac preparations. (*A*) Twitch contractions of rat left atria electrically stimulated at 1 Hz. Development of the negative inotropic effect in the presence of 1 μM CaC. (*B*) Dose–response curve for the action of CaC on the L-type Ca^{2+} current in rat cardiac cells (●) and the twitch contraction in rat left atria (○). (*C*) (*a*) T- and L-type Ca^{2+} currents evoked in voltage-clamped rat cardiac cells in primary culture from holding potential (HP) = −80 mV by a double-pulse protocol. (*b*) Control T- and L-type currents. (*c*) Specific blockade of the L-type current after a 10-min application of 25 nM CaC. Recovery of the L-type current was never observed even after a 30-min washout of the toxin (data not shown). (*D*) Peak current–voltage (*I–V*) plots from a rat cardiac cell in the absence (●) and in the presence (▲) of 0.1 μM CaC; HP = −80 mV. (*E*) Mouse skeletal muscle in primary culture. Ca^{2+} currents in response to a step depolarization to 0 mV from HP = −90 mV (upper traces) and associated contractions (lower traces) obtained in the absence of CaC and after a 10-min application of 1 μM CaC.

currents of rat cardiac cells in primary culture were studied simultaneously by using a double-pulse protocol (Fig. 2*Ca*). Application of 25 nM CaC has no effect on the T-type current, while it nearly blocks the L-type current (Fig. 2*C b* and *c*). Fig. 2*D* shows that CaC selectively blocks the L-type current and therefore unmasks the *I–V* relationship for the T-type Ca^{2+} current. The half-blocking concentration of CaC is 5 nM (n = 5) (Fig. 2*B*). The negative inotropic effect of CaC is correlated to the degree of block of the cardiac L-type Ca^{2+} current.

In rat and mouse skeletal muscle cells in primary culture, neither the T-type current nor the L-type current nor contraction associated to the voltage-sensor function (27, 28) was affected by application of 1 μM CaC (Fig. 2*E*).

In all neuronal preparations tested (chicken and rat DRG cells, cerebellar rat Purkinje and granule cells), the T-type channels were unmodified by 0.1–1 μM CaC (data not shown).

The HVA current of chicken DRG neurons is essentially composed of L- and N-type currents (29). The cells were first exposed to saturating concentrations of either PN (1 μM), a DHP, or CgTx (1 μM) to "isolate" N- or L-type Ca^{2+} channels, respectively, before applying CaC at a concentration of 100–200 nM (Fig. 3 *A* and *B*). The toxin blocked both neuronal L- and N-type channels with similar potencies (n = 42). Fig. 3*C* shows the dose dependency of the block of the Ca^{2+} current by CaC (EC_{50} = 25 nM; n = 18). Rat DRG neurons contain a fraction (20–30%) of high-threshold current resistant to both DHPs and CgTx (30). In all rat DRG neurons (n = 15) tested in the absence (Fig. 3*D*) or in the presence of 1 μM PN (Fig. 3*E*) or 1 μM CgTx (Fig. 3*F*) or both, ≈20% of the Ca^{2+} current remained unblocked after a 5- to 10-min

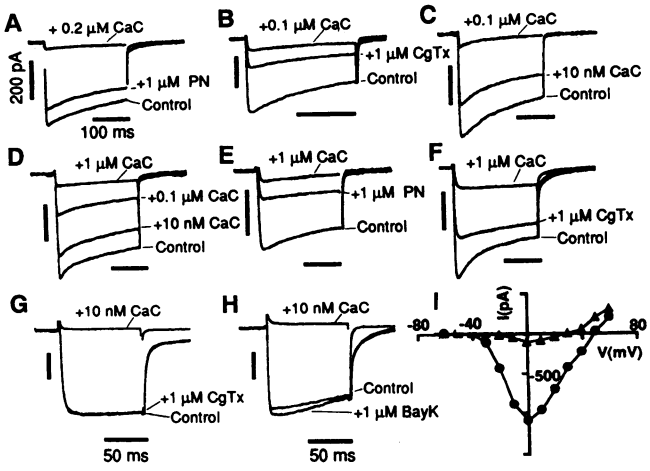

FIG. 3. Effect of CaC on neuronal preparations. (*A–C*) Chicken DRG neurons. Superimposed traces of Ca^{2+} currents evoked by depolarizing pulses to 0 mV from holding potential (HP) = −80 mV. (*A*) Inhibition of current by 1 μM PN alone and by 1 μM PN plus 0.2 μM CaC. (*B*) Inhibition of current by 1 μM CgTx and by 1 μM CgTx plus 0.1 μM CaC. (*C*) Effect of increasing concentrations of CaC on the Ca^{2+} current; 10-min exposure to each concentration. (*D–F*) Rat DRG neurons. (*D*) Dose-dependent block of the Ca^{2+} current by CaC; same procedure as in *C*. (*E* and *F*) Incomplete block of the PN- (*E*) and CgTx- (*F*) insensitive Ca^{2+} currents by 1 μM CaC. (*G–I*) Rat cerebellar Purkinje neurons. (*G*) Sequential applications of CgTx and CaC; absence of effect of 1 μM CgTx and complete block of the current after a 10-min exposure to 10 nM CaC. (*H*) Sequential applications of Bay K8644 and CaC; small increase of the current in the presence of 1 μM Bay K8644 and complete block after a 10-min addition of 10 nM CaC. Superimposed traces of current evoked by depolarizing pulses to 0 (*G*) or −10 (*H*) mV from HP = −80 mV. (*I*) Peak current–voltage (*I–V*) plots in the absence (●) and in the presence (▲) of 10 nM CaC. External medium contained 5 mM Ba^{2+}. Horizontal bars, 100 ms; vertical bars, 200 pA.

application of 1 μM CaC. Fig. 3*D* shows the dose-dependent inhibition of the HVA current by CaC. The CaC-sensitive Ca^{2+} current has an EC_{50} value for inhibition of 60–80 nM.

Effects of CaC on P-type channels were tested on rat cerebellar Purkinje neurons in which the majority of the HVA current (>90%) is of the P-type (3). Fig. 3 *G* and *H* confirm that these cells do not contain significant CgTx- and DHP-sensitive Ca^{2+} currents. CaC blocks the P-type current (Fig. 3 *G–I*) with an EC_{50} value of 1–5 nM and complete block occurs at 10–50 nM (n = 10).

The concentration of ^{125}I-CaC used in the autoradiographic procedure corresponds to the K_d value (35 pM) determined in preliminary binding experiments on rat brain microsomes (see Fig. 5*A Lower Inset*). The distribution of specific CaC binding sites throughout rat brain is heterogeneous (Fig. 4 *A–E*). In the olfactory bulb, the glomeruli and the internal granular layer have the highest density of CaC binding sites, as compared to the plexiform layer (Fig. 4*A*). All regions of cerebral cortex are labeled with the highest density in layers I, II, and IV (Fig. 4 *B–D*). In the basal ganglia, high densities of CaC sites are found in the accumbens nucleus and the caudate putamen; a low density is seen in globus pallidus (Fig. 4 *B* and *C*). All nuclei of amygdala are highly labeled (Fig. 4*D*). In the hippocampal formation (Fig. 4*D*), the molecular layer of the dentate gyrus and the stratum oriens of CA3 field show a high level of labeling, while the stratum radiatum and the hilus present a moderate level. The pyramidal cell layer and the stratum lacunosum moleculare are weakly labeled. All nuclei of the thalamus, particularly the ventroposterior thalamic and the geniculate nuclei, are highly labeled. The habenula is not labeled. The hypothalamus is weakly labeled except in the arcuate hypothalamic nucleus. In the midbrain, the superficial grey layer of superior colliculus showed the largest density of CaC sites. In the hindbrain, the trapezoid bodies, the pontine nuclei, the raphe pontis, and the inferior olive are labeled. The granular layer of the cerebellum contains the highest level of labeling while the molecular layer is not labeled (Fig. 4*E*). The cytolocalization of CaC binding sites in cerebellum was examined by using neurological mutant mice with selective deficiencies in the cerebellar cortex (Fig. 4 *G–L*). Weaver mice, which are depleted of cerebellar granule and Purkinje cells (Fig. 4*G*), show an important decrease of labeling (Fig. 4*H*). The Reeler mutant has an atrophied molecular layer, a reduced granular layer, and an incomplete monolayer of Purkinje cells (Fig. 4*I*). In that case, CaC binding sites were strictly located in granular cells (Fig. 4*J*). The Purkinje cell degeneration mouse cerebellum has an important loss of Purkinje cells (Fig. 4*K*). The distribution of CaC binding sites looked very similar to that of normal cerebellum (Fig. 4*L*). All these results show that CaC sites are essentially associated with cerebellar granule cells.

^{125}I-CaC binds to olfactory bulb microsomes with a high affinity corresponding to K_d = 15 pM and B_{max} = 92 fmol per mg of protein (Fig. 5*A*). A $K_{0.5}$ value of 49 pM was found from the inhibition of ^{125}I-CaC binding by cold CaC giving a calculated K_d of 36 pM (Fig. 5*B*). Six classes of molecules are known to specifically block the L-type Ca^{2+} channels (5, 31), the DHPs (PN), benzothiazepines (diltiazem), phenylalkylamines (D600), diphenylbutylpiperidine (fluspirilene), benzolactam (HOE166), and indolizinsulfones (SR 33557). None of these blockers of the L-type Ca^{2+} channel and CgTx, up to 1 μM, inhibited the binding of ^{125}I-CaC to olfactory bulb microsomes (Fig. 5*B*). ^{125}I-CaC binding sites are absent (data not shown) in skeletal muscle T-tubules, which are very rich in DHP receptors (5).

In cerebellar granule cells, which contain high levels of ^{125}I-CaC binding sites (Fig. 4*E*), a component of the Ca^{2+} current is of the L-type (18), but a CgTx-sensitive current and a current resistant to both DHP and CgTx are also present

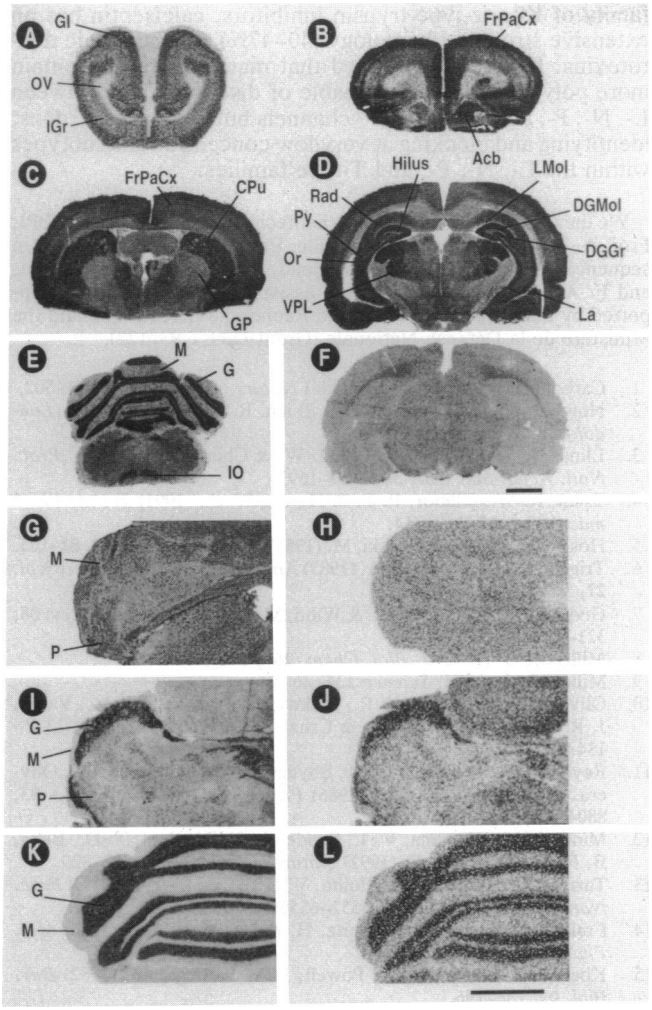

FIG. 4. Distribution of CaC binding sites in normal rat brain (*A–E*) and in cerebellum of mutant mice (*G–L*). Coronal sections were incubated in 35 pM ^{125}I-CaC for total binding or in the presence of 0.1 μM unlabeled CaC for nonspecific binding (*F*). Dark areas represent high densities of CaC binding sites from Wistar rat (*A–E*), Weaver (*H*), Reeler (*J*), and Purkinje cell degeneration (*L*) mice. (*G*, *I*, and *K*) Corresponding Giemsa-stained tissue sections of mutant mice. Distribution of CaC binding sites is identical in the cerebellum of rat (*E*) and of wild-type mice (data not shown); therefore, *E* should also be seen as a control for studies with mutant mice. Acb, accumbens nucleus; CPu, caudate putamen; DGGr, granular layer of dentate gyrus; DGMol, molecular layer of dentate gyrus; FrPaCx, frontoparietal cortex; G, granular layer of cerebellum; Gl, glomerular layer of olfactory bulb; GP, globus pallidus; Hilus, hilus of dentate gyrus; IGr, internal granular layer of the olfactory bulb; IO, inferior olive; La, lateral amygdaloid nucleus; LMol, stratum lacunosum moleculare; M, molecular layer of cerebellum; Or, stratum oriens of Ammon's horn; OV, inferior olive; P, Purkinje cell layer; Py, pyramidal cell layer of Ammon's horn; Rad, stratum radiatum of Ammon's horn; VPL, ventroposterior thalamic nucleus. (*B–L*, bar = 1 mm; *A*, bar = 2 mm.)

(32). Fig. 6*A* shows that block of the Ca^{2+} current by CaC is dose dependent but incomplete; 90% of the CaC-sensitive Ca^{2+} current is blocked by 1 nM toxin and the EC_{50} for the inhibition is 0.2 nM (n = 8). Fig. 6*D* confirms the existence of a substantial L component since PN (1 μM) produces a clear reduction of the current. Fig. 6*B* shows that CgTx blocks a fraction of the total current comparable to that blocked by PN. After cerebellar granule cells were exposed sequentially to a saturating concentration of CaC (0.1 μM) and CgTx (1 μM), application of PN (1 μM) had no additional effect, implying that CaC totally blocked L-type channels

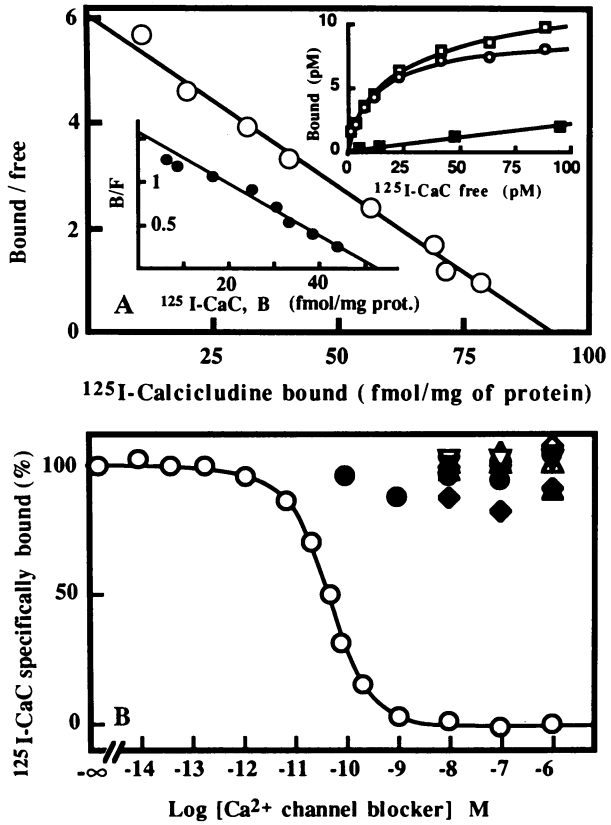

FIG. 5. (*A*) Binding of ^{125}I-CaC to rat olfactory bulb microsomes. (*Main Panel* and *Upper Inset*) Membranes (0.1 mg of protein per ml) were incubated with ^{125}I-CaC (3–100 pM). (*Upper Inset*) Saturation curve for ^{125}I-CaC specific binding (○) obtained after subtraction of nonspecific ^{125}I-CaC binding (■) (determined by including 10 nM CaC in the incubation medium) from the total ^{125}I-CaC binding (□). (*Main Panel*) Corresponding Scatchard plot (○). Results are means of two determinations. Bound/free is expressed as pmol/(mg of protein × nM). (*Lower Inset*) Binding of ^{125}I-CaC to rat brain microsomes. Scatchard plot of the data. (*B*) Dose–response curve of inhibition by CaC and different Ca^{2+}-channel blockers of specific ^{125}I-CaC binding to rat olfactory bulb microsomes. Unlabeled CaC and Ca^{2+}-channel blockers were first incubated at different concentrations with the membranes (0.1 mg/ml) and then ^{125}I-CaC (6 pM) was added and membranes were incubated for 1 hr. Results are means of two experiments. ○, CaC; ●, CgTx; ◇, PN; ◆, diltiazem; △, SR 33557; ▲, HOE166; ▽, fluspirilene; ▼, D600.

(Fig. 6*C*). When cells were first exposed to PN, subsequent addition of CaC (0.1 μM) blocked only a small component of current (Fig. 6*D*). So CaC potently and specifically blocks L-type Ca^{2+} channel in cerebellar granule cells.

DISCUSSION

CaC is a 60-amino acid peptide with three disulfide bridges. It is a potent and specific inhibitor of high-threshold Ca^{2+} channels in a variety of excitable cells. Nevertheless, the sensitivity of L-, N-, and P-type Ca^{2+} channels to this toxin is clearly tissue- and species-dependent. For instance, rat cerebellar granule cell L-type channels are much more sensitive to CaC (EC_{50} = 0.2 nM) than rat cardiac L-type channels (EC_{50} = 5 nM) and rat peripheral DRG neuronal L-type channels (EC_{50} = 60–80 nM). A total insensitivity was found for rat skeletal muscle L-type channels. Chicken DRG N-type channels are more sensitive to CaC (EC_{50} = 25 nM) than rat DRG N-type channels (EC_{50} = 60–80 nM). Cerebellar granule cell N-type channels are almost insensitive to CaC (EC_{50} > 100 nM). HVA Ca^{2+} currents resistant to both DHPs and CgTx, which have been observed in rat DRG neurons and cerebellar granule cells, were generally insen-

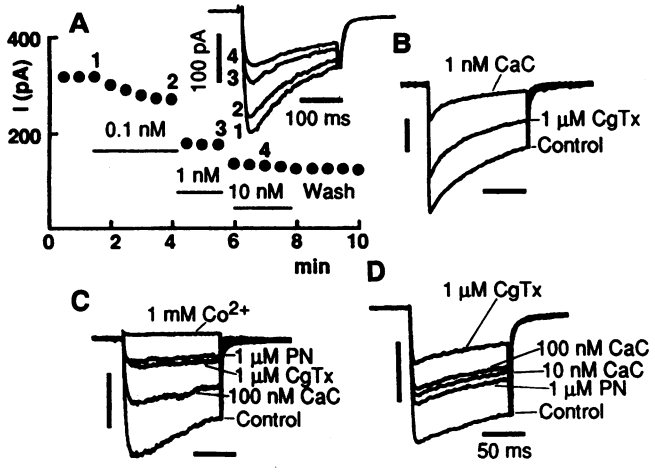

FIG. 6. Effect of CaC on rat cerebellar granule cells. Superimposed traces of Ca^{2+} currents evoked by depolarizing pulses to 0 mV from holding potential = −80 mV. (*A*) Time course of inhibition of the peak current after application of CaC at increasing concentrations. (*Inset*) Traces at the time points indicated. (*B*) Effect of CaC on CgTx-insensitive component of the current. Control, after a 1-min exposure to 1 μM CgTx, and then stationary effect of 1 nM CaC. (*C*) Selective inhibition of L-type current by CaC. Control, effect of a saturating concentration of CaC (100 nM), followed by application of 1 μM CgTx. Addition of 1 μM PN did not affect appreciably the remaining current. Complete blockade of the current by 1 mM Co^{2+}. (*D*) Effect of CaC on the DHP-insensitive component of the current. Control, application of 1 μM PN. Small inhibitory effects of 10 and 100 nM CaC on the DHP-insensitive component of the current. A noticeable part of the remaining current was then blocked by 1 μM CgTx. Control Ca^{2+} currents could be recorded for >20 min without significant rundown by adding cAMP in the pipette solution (18). Horizontal bars, 100 ms; vertical bars, 200 pA.

sitive to CaC. P-type currents in cerebellar Purkinje cells have a good sensitivity to CaC blockade (EC_{50} = 1–5 nM). CaC is the only ligand described capable of blocking L-, N-, and P-type Ca^{2+} channels. It appears also to be a selective blocker of a subtype of L-type Ca^{2+} channel that is predominantly expressed in cerebellar granule cells.

Binding experiments on rat olfactory bulb membranes using ^{125}I-CaC have identified a single class of high-affinity binding sites with a K_d of 15–36 pM. These constitute a class of binding sites distinct from and without interactions with those of the classical classes of L- or N-type Ca^{2+}-channel blockers. Comparative distributions of ^{125}I-CaC binding sites in cerebellum mutants (Weaver, Reeler, Purkinje cell degeneration) with different cellular deficits have clearly shown that these sites are located in cerebellar granule cells. These high-affinity binding sites are most likely associated with L-type Ca^{2+} channels expressed in cerebellar granule cells. It is probable that the high-affinity binding sites for CaC present in other areas of the brain correspond to the Ca^{2+}-channel subtype identified in cerebellar granule cells.

The CaC structure has evident structural homologies with dendrotoxins, basic pancreatic trypsin inhibitor, and APPI (Fig. 1), three peptides that have the same folding pattern (33–35). Future modifications of the CaC structure will permit delineation of the sequence properties that make it a Ca^{2+}-channel blocker, while dendrotoxins are K^+-channel inhibitors. These two types of toxins, in spite of their similar structure, have no mutual interaction. CaC does not alter ^{125}I-dendrotoxin I binding to brain membranes and dendrotoxin I does not alter ^{125}I-CaC binding. APPI has no effect on ^{125}I-CaC binding (data not shown).

Another 60-amino acid protein with L-type Ca^{2+}-channel blocking activity, called calciseptin, has been isolated from *Dendroaspis polylepis* (36). While CaC belongs to the superfamily of Kunitz-type trypsin inhibitors, calciseptin has an extensive structural homology (40–47%) with nicotinic neurotoxins. It is to be expected that mamba venoms contain more polypeptide toxins capable of discriminating between L-, N-, P-, and T-type Ca^{2+}-channels but also, as CaC does, identifying and blocking at very low concentrations subtypes within the L-, N-, P-, and T-type families.

We thank Dr. R. A. Lazarus (Genentech) for the kind gift of APPI; Prof. A. Tartar (Institut Pasteur, Lille, France) for his useful help in sequence determination; and V. Friend, C. Widmann, C. Roulinat, and F. Aguila for expert technical assistance. This work was supported by the Centre National de la Recherche Scientifique and the Ministère de la Défense Nationale (Grant DRET 93/122).

1. Carbone, E. & Lux, H. D. (1984) *Nature (London)* **310**, 501–502.
2. Nowycky, M. C., Fox, A. P. & Tsien, R. W. (1985) *Nature (London)* **316**, 440–443.
3. Llinas, R., Sugimori, M., Liu, J. W. & Cherksey, B. (1989) *Proc. Natl. Acad. Sci. USA* **86**, 1689–1693.
4. Tsien, R. W., Ellinor, P. T. & Horne, W. A. (1991) *Trends Pharmacol. Sci.* **12**, 349–354.
5. Hosey, M. M. & Lazdunski, M. (1988) *J. Membr. Biol.* **104**, 81–105.
6. Triggle, D. J. & Janis, R. A. (1987) *Annu. Rev. Pharmacol. Toxicol.* **27**, 347–369.
7. Godfraind, T., Miller, R. J. & Wibo, M. (1986) *Pharmacol. Rev.* **38**, 321–416.
8. Miller, R. J. (1992) *J. Biol. Chem.* **267**, 1403–1406.
9. Miller, R. J. (1987) *Science* **235**, 46–52.
10. Olivera, B. M., Gray, W. R., Zeikus, R., McIntosh, J. M., Varga, J. Rivier, J., de Santos, V. & Cruz, L. (1985) *Science* **230**, 1338–1343.
11. Reynolds, I. J. Wagner, J. A., Snyder, S. H., Thayer, S. A., Olivera, B. M. & Miller, R. J. (1986) *Proc. Natl. Acad. Sci. USA* **83**, 8804–8807.
12. Mintz, I. M., Venema, V. J., Swiderek, K. M., Lee, T. D., Bean, B. P. & Adams, M. E. (1992) *Nature (London)* **355**, 827–829.
13. Tarr, G. E., Black, S. D., Fujita, V. S. & Coon, M. J. (1983) *Proc. Natl. Acad. Sci. USA* **80**, 6552–6556.
14. Frelin, C., Vigne, P., Schweitz, H. & Lazdunski, M. (1984) *Mol. Pharmacol.* **26**, 70–74.
15. Koenig, J., Bournaud, R., Powell, J. A. & Rieger, F. (1982) *Dev. Biol.* **92**, 188–196.
16. Dunlap, K. & Fischbach, G. D. (1981) *J. Physiol. (London)* **317**, 519–535.
17. Hockberger, P. E., Tseng, H.-Y. & Connor, J. A. (1989) *J. Neurosci.* **9**, 2258–2271.
18. Slesinger, P. A. & Lansman, J. (1991) *J. Physiol. (London)* **435**, 101–121.
19. Hamill, O. P., Marty, A., Neher, E., Sakmann, B. & Sigworth, F. J. (1981) *Pflügers Arch.* **391**, 85–100.
20. Renaud, J. F., Fosset, M., Schweitz, H. & Lazdunski, M. (1986) *Eur. J. Pharmacol.* **120**, 161–170.
21. Mourre, C., Cervera, P. & Lazdunski, M. (1987) *Brain Res.* **417**, 21–32.
22. Moczydlowski, E., Lucchesi, K. & Ravindran, A. (1988) *J. Membr. Biol.* **105**, 95–111.
23. Dreyer, F. (1990) *Rev. Physiol. Biochem. Pharmacol.* **115**, 93–136.
24. Reuter, H. (1983) *Nature (London)* **301**, 569–574.
25. Nilius, B., Hess, P., Lansman, J. B. & Tsien, R. W. (1985) *Nature (London)* **316**, 443–446.
26. Bean, B. P. (1985) *J. Gen. Physiol.* **86**, 1–30.
27. Ma, J., Mundina-Weilenmann, C., Hosey, M. M. & Rios, E. (1991) *Biophys. J.* **60**, 890–901.
28. Bois, P., Romey, G. & Lazdunski, M. (1991) *Pflügers Arch.* **419**, 651–656.
29. Aosaki, T. & Kasai, H. (1989) *Pflügers Arch.* **414**, 150–156.
30. Regan, L. J., Sah, D. W. Y. & Bean, B. P. (1991) *Neuron* **6**, 269–280.
31. Rampe, D. & Triggle, D. J. (1990) *Trends Pharmacol. Sci.* **11**, 112–115.
32. Haws, C. M., Slesinger, P. A. & Lansman, J. B. (1993) *J. Neurosci.* **13**, 1148–1156.
33. Foray, M. F., Lancelin, J. M., Hollecker, M. & Marion, D. (1993) *Eur. J. Biochem.* **211**, 813–820.
34. Skarzynski, T. (1992) *J. Mol. Biol.* **224**, 671–683.
35. Hynes, T. R., Randal, M., Kennedy, L. A., Eigenbrot, C. & Kossiakoff, A. (1990) *Biochemistry* **29**, 10018–10022.
36. De Weille, J. R., Schweitz, H., Maes, P., Tartar, A. & Lazdunski, M. (1991) *Proc. Natl. Acad. Sci. USA* **88**, 2437–2440.